Post-Print

This is the accepted version of:

M. Anghileri, L.M. Castelletti, E. Francesconi, A. Milanese, M. Pittofrati
Survey of Numerical Approaches to Analyse the Behavior of a Composite Skin Panel During a Water Impact
International Journal of Impact Engineering, Vol. 63, N. 1, 2014, p. 43-51
doi:10.1016/j.ijimpeng.2013.08.008

The final publication is available at https://doi.org/10.1016/j.ijimpeng.2013.08.008

Access to the published version may require subscription.

Survey of numerical approaches to analyse the behavior of a composite skin panel during a water impact

Marco Anghileri, Luigi-Maria L. Castelletti, Edoardo Francesconi,
Andrea Milanese, Michele Pittofrati

Politecnico di Milano, Dipartimento di Scienze e Tecnologie Aerospaziali, Via La Masa 34, 20156 Milan, Italy

Abstract

Water impacts may have tragic consequences for the passengers of helicopters. Most of the passive safety devices developed for helicopter crashworthiness is designed for ground impact. The loading that characterizes the impact with hard and soft surfaces is different and therefore energy absorption devices developed for ground impact are not effective during a water impact.
Various researches focus on the use of composite materials for aircraft and helicopter fuselage. In this paper, in particular, it is investigated the behavior of a composite panel during the impact with water and the approaches to study the event by means of finite element codes.
In order to collect reliable data for numerical model validation, water impact drop tests were carried out. A sample panel, made with a Carbon Fiber Reinforced Plastic material similar to those used for modern aircraft skin panels, was manufactured. A specific test device was created and used in the tests. Impact decelerations and deformation of the panel were measured.
Numerical models of the tests were created. Meshless approaches were used, in addition to Lagrangian and Eulerian Finite elements, to model the water region. Eventually, a close experimental–numerical correlation was obtained for each model in terms of impact dynamics, decelerations and composite panel deformation. The main features of the event and the differences between the four numerical approaches were discussed. Guidelines for further investigations were also drawn.

Introduction

Water impact is an issue of great importance for rotorcraft and aircraft crashworthiness. Statistics [1] has shown that 10% of civil aircraft accidents and 25% of military aircraft accidents involve impacts with water.
While remarkable progresses in crashworthiness design have been achieved in recent years, most of the passive safety devices have been developed considering ground impacts [2]. Analyzing the structure behavior during a ground impact versus a water impact, experience shows that the load paths are completely different (Fig.1). Therefore, it is not unusual that energy absorption devices designed for ground impact are not effective during a water impact.

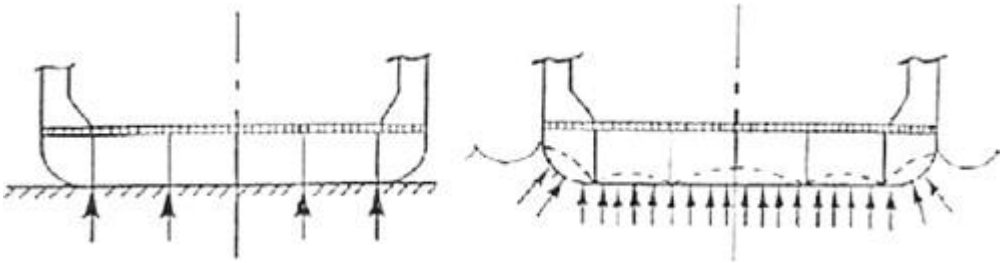

Fig. 1. Ground impact (left) vs. water impact (right)[3].

Impact loads during a water impact are usually lower with respect to equivalent ground impact scenarios, but the impact duration is longer and load distribution involves parts of the structure not designed to carry impact loads [3].
When an aircraft is involved in a ground crash landing the load is transferred through subfloor structure (frames and spars), which absorbs part of the impact energy by progressively deforming. Since ground deformation can be considered negligible with respect to the structure, the load entity and path is more predictable and a crashworthy design of the aircraft subfloor can be developed to limit the loads transmitted to the occupants.
On the contrary, when an aircraft is involved in a water landing, the water pressure impinging on the skin panels leads to panels collapse and consequent failure of the load transfer mechanism between skin panels and subfloor structure, affecting the energy absorption capabilities of the subfloor. The skin panels collapse leads to two potentially critical consequences: reduction of the energy absorption capability of subfloor and water inrush with consequent cabin flood and reduction of floating time.
The analysis of the event before the failure of the panel is complicated by the fact that the entity of the impact loads also depends on fluid–structure interaction.
At Politecnico di Milano Laboratory for Safety in Transports (LAST) research activities on fluid–structure interaction and helicopter ditching have been performed since 1994. Between 2005 and 2008 it joined the Group for Aeronautical Research and Technology in Europe (GARTEUR) AG15 was established to improve the Smoothed Particle Hydrodynamics (SPH) method for application to helicopter ditching.
Following previous research work on non-deformable bodies impacting water [4], the activity was focused on fluid–structure interaction between water and a composite Carbon Fiber Reinforced Plastic (CFRP) skin panel.
The research work consisted of two phases: the initial experimental phase and the subsequent numerical phase.
In the experimental phase, water impact drop test were carried out to collect test data to develop and validate numerical models. An instrumented CFRP flat panel was mounted on a specifically built test frame, during the tests both decelerations on the frame and deformations of the panel were measured.
In the numerical phase the tests were reproduced modeling the fluid region with different numerical formulations; two finite elements approaches, Lagrangian and ALE, and two *meshless* formulations, SPH and EFG. LSTC LS-Dyna 971 [5], a proven and commercially-available nonlinear explicit finite element code was used. The results obtained were compared against experimental tests and to evaluate different formulations performances in terms of correlation and computational efficiency, providing important guidelines for modeling fluid–structure interaction in water impact events.

Experimental tests

The intense test campaign carried out in the first part of the research consisted of performing water impact drop tests using a CFRP skin panel.
A solid test frame was built to investigate the impact behavior of the panel. During the tests impact decelerations and deformations were acquired. Besides, high velocity movies of the tests were recorded to evaluate the impact dynamics of the event.

The specimen

The specimen (Fig.2) was a flat 400 × 400 mm CFRP panel. The panel was made with Vicotex 914/42%/G803 (carbon fiber woven 42% in resin epoxy) and a stacking sequence [90°, 45°, 0°, −45°]$_{SYM}$ typical of some aircraft skin panels were used. The nominal thickness of the panel was 2.00 mm.

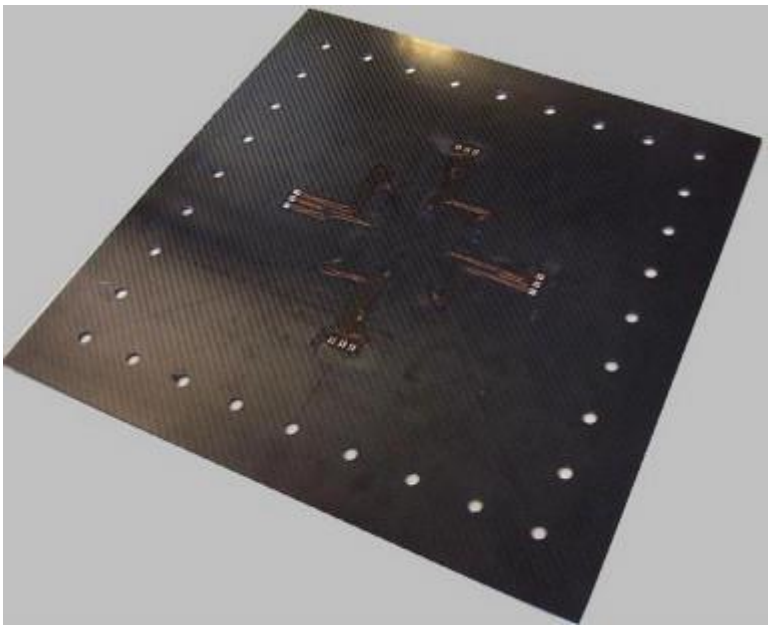

Fig. 2. The CFRP skin panel.

The test article

The test article (Fig.3) consisted of a massive base frame, four lateral flat Aluminum alloy panels and L-shaped corner stiffeners. The base frame, in particular, was a 400 × 400 mm, 40-mm height Al 6082-Ta16 plate machined to have a square hole of 320 × 320 mm. The CFRP panel was bolted on the base frame so that the actual impact region was 320 × 320 mm.

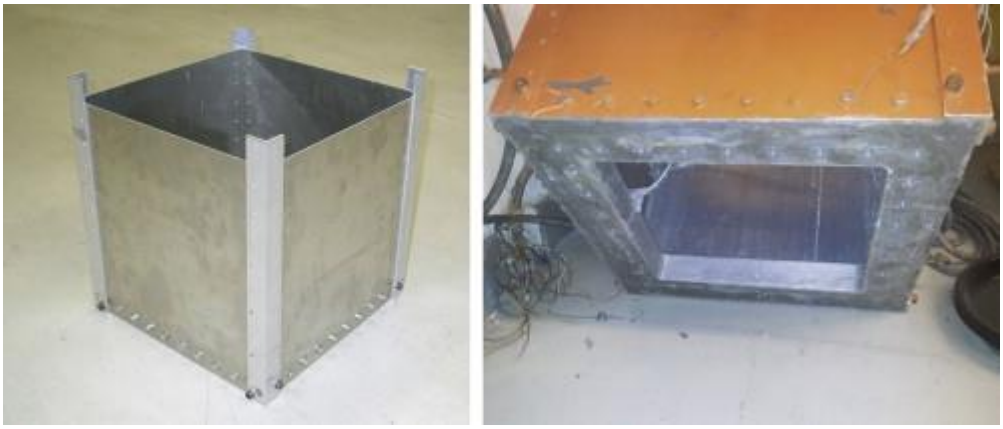

Fig. 3. The test frame panels (left) and base (right).

The test article was provided with a cap to avoid water inrush. The global dimensions of the test article were 400 × 400 × 500 mm and the test mass was 16.9 kg including instrumentation, cap and cables. Most of the weight of the test article was due to the frame so that the center of mass was located at the bottom of the test frame. The lateral panels were added to avoid sinking after the water impact and to provide a more solid connection to the guide used to guarantee a constant, zero-angle

incidence of the test article during the fall. These panels, 2.0 mm thick, were designed to provide the necessary stiffness to the structure and to be lighter than the base frame.
The test frame was designed to test panels of different materials and thicknesses and to focus the analysis only on the panel behavior.

Test facility

The dimensions of the test article allowed performing the drop tests using the indoor facilities of LAST. A 3000 kg bridge crane was used as hoisting system and a 1.5-m diameter and 1.4-m depth PVC round pool was used as water basin.
The test article was hanged to a quick-release system and four steel cables were used to guide the test article during the fall and to maintain the impact incidence of the test article within acceptable limits (i.e. smaller than 3°). The test facility is shown in [Fig.4].

Fig. 4. The test facility.

Instrumentation

Impact decelerations and deformations were measured during the tests because they are quantities of great interest in designing structures safe in water landing.

Accelerometers

Four ENTRAN D-0-500 accelerometers were used to measure impact decelerations. The accelerometers were fixed in the midpoints of the sides of the base frame (Fig.5). The number and the pattern of the accelerometers allowed a sufficient redundancy of the measurements and the possibility to evaluate the impact incidence of the test article.

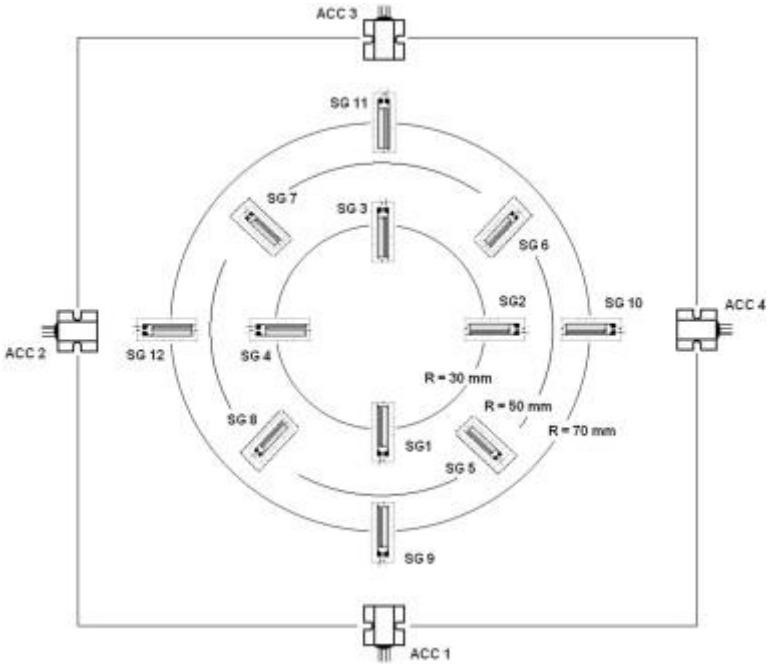

Fig. 5. The transducer configuration.

Strain gauges

Twelve OMEGA KFG-5-120 strain gauges with 5 mm gauge length were installed on the skin panels to measure impact deformations. The strain gauges were placed on three circumferences of radius respectively of 30 mm, 50 mm and 70 mm – as shown in Fig.5. The number and the placement of the strain gauges allowed to have redundancy in the measurements and to evaluate the deformation in different points of the panel accordingly with the shape of the deformation of the panel itself. The strain gauges were sealed to avoid contact with water.

High speed camera

The tests were filmed using a high speed camera to capture the impact dynamics of the event and to have a deeper insight in it. The movies were also used to estimate the impact velocity and the incidence of the test article.

Data acquisition system

The accelerometers and the strain gauges were connected to a Power-DAQ 14 bit/16 channels data acquisition system. Signals were acquired at 20,000 Hz to avoid aliasing and to guarantee a large number of sample points during the initial phase of the impact, when the quantities of interest change rapidly. The value of the sampling rate was also decided in view of evaluating the delay between the accelerometers pulses.

Tests performed

The water impact tests were carried out releasing the test article from several prescribed heights. The facility used in the tests allows a maximum drop height of 3.0 m. Nevertheless, to avoid delamination or cracks of the skin panel under investigation, the maximum drop height was limited to 1.50 m, X-ray radiographic images of the skin panel confirmed that no delamination or permanent damage was present after the testing.

Measured impact velocities and analytical predictions based on weight drop showed that the influence of the friction of the guides was negligible (the difference was smaller than 3%). Carried out tests and measured impact velocities are listed in Table 1.

Test #	Drop height [m]	Impact velocity [m/s]
1	0.10	1.29
2	0.30	2.29
3	0.50	3.12
4	0.70	3.67
5	1.00	4.35
6	1.30	4.96
7	1.50	5.32

Table 1. Tests carried out, drop heights and estimated impact velocities.

For every height, the tests were repeated at least five times to ensure the accuracy of the measures and to verify the repeatability of the data acquired.
The impact incidence of the test article was evaluated on the basis of both high speed movies (Fig.6) and differences in acquired decelerations (pulse values and time delays). Only the tests with an impact incidence smaller than 3° were considered acceptable and therefore the number of tests carried out was larger than the one suggested from Table 1.

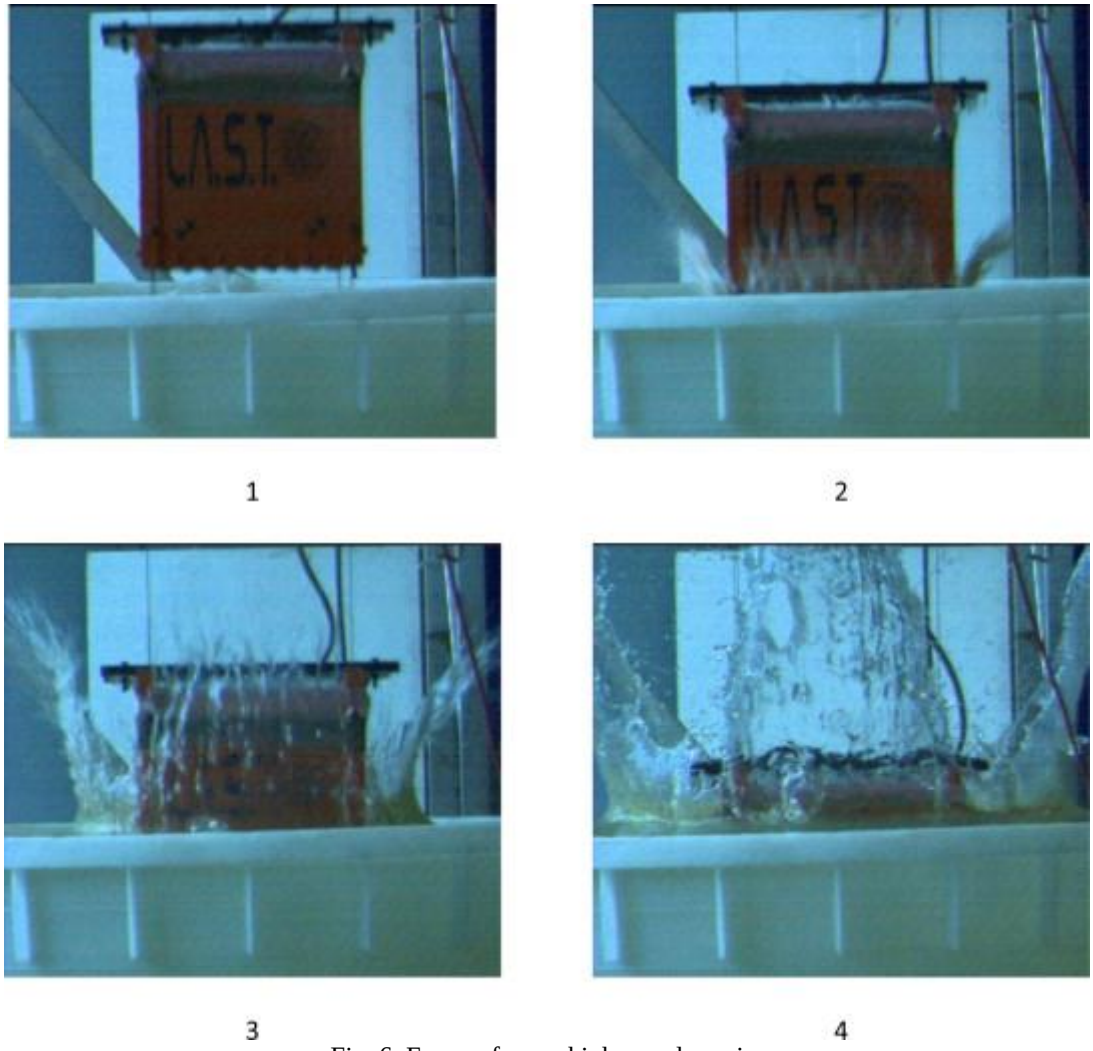

Fig. 6. Frames from a high speed movie.

Data collected

The impact deceleration time history for three reference drop heights is plotted in Fig.7. Inspecting Fig.7, it is possible to infer the general trend of the decelerations: a first peak and the following oscillations due to the test article dynamic response. The deceleration time history for each test has been computed as an average of the output of the transducers; the test time histories thus obtained have been averaged for tests of the same drop height in order to elaborate the reference curves reported in Fig.7. A similar procedure has been used for the deformation. The deformation time history of the CFRP skin panel for three reference drop heights, plotted in Fig.8, is measured with quarter bridge configuration and reported in micro-strain.

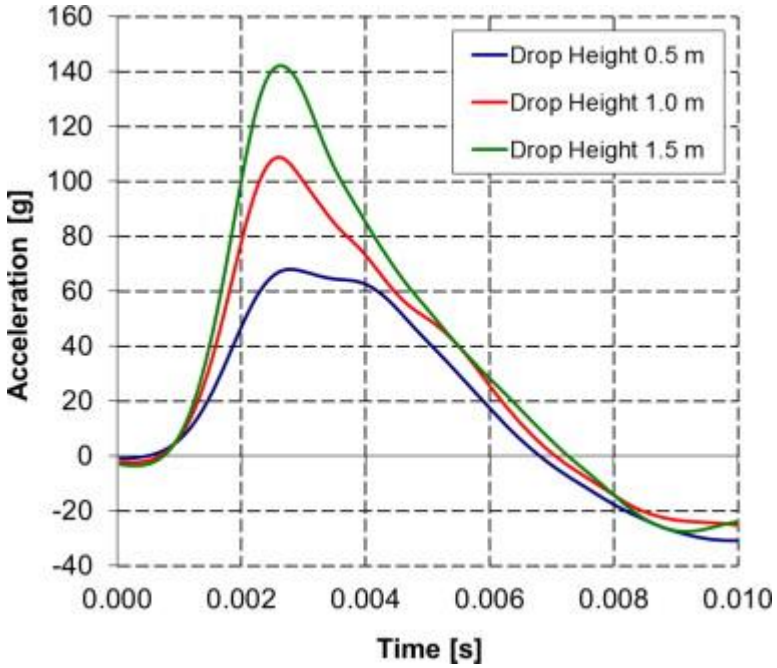

Fig. 7. Impact decelerations.

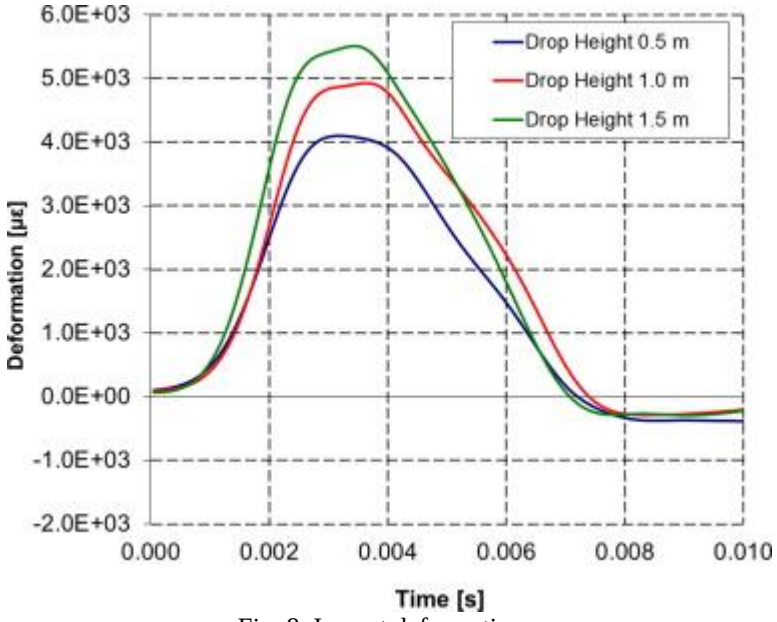

Fig. 8. Impact deformations.

Inspecting Fig.8, it is possible to observe the general trend of the deformations: a first peak and the following oscillations due to the base panel vibrations.

Remarks

The repeatability of the tests in terms of collected data indicates the reliability of the carried out tests. In effort to compare the mean measurements obtained in the tests from different drop heights, the acquired data were also made dimensionless according to Ref.[6]:where v_i is the impact velocity, ρ_w is the density of water while M_p, S_p and L_p are the mass, impact surface area and width of the test article.
The mean values of the decelerations and deformations are shown in Figs. 7 and 8 the standard deviation from the mean values is negligible for all the tests carried out in the two campaigns.
The impact decelerations and deformations for different drop heights were compared all together observing a linear trend with respect to the impact velocity, as a consequence, the dimensionless peaks decreased with the drop height.

Numerical simulations

The second phase of the research was devoted to develop and validate reliable numerical models of the carried out tests.
The Lagrangian FE approach was adopted to model the test article whilst the fluid region was modeled adopting four different approaches: Lagrangian FE, ALE, SPH and EFG. Despite its known drawbacks, the Eulerian approach is usually preferred in fluid modeling to the Lagrangian FE one because it allows handling severe deformations without significant accuracy reduction. The drawbacks in the use of the Eulerian formulation stimulate researches on different solutions of the problem such as meshless methods based on the Lagrangian approach. SPH is a genuinely meshless method initially introduced in astrophysics [7] and subsequently applied to a number of Continuum Mechanics problems such as events involving fluid–structure interaction or high velocity impacts. EFG method was first introduced to study crack propagations [8] and its applications to fluid–structure interaction are still quite rare. The feasibility of each model was investigated and the accuracy quantitatively evaluated referring to the data collected in the tests – i.e. test article decelerations and base panel deformations.
The model exploited the double symmetry of the problem and only a quarter of both the test article and the fluid region were modeled. Proper symmetry constraints were applied both to the Lagrangian model and the water region.

Finite elements model of the test article

The test specimen was a square flat composite panel and hence it was possible to build a regular and uniform mesh consisting of 3600 four-node shell elements. The reference length of the elements (about 6.6 mm) was a trade-off between accuracy and CPU-time required by the simulations and was decided on the characteristic dimension of the elements in the fluid region.
The panel was modeled as a laminate accordingly with the Classic Lamination Theory that allows modeling the stacking sequence and the fiber orientations of each ply in the laminate. One integration point for each ply was defined.
The composite material was modeled using a constitutive law based on the Damage Mechanics for which it is assumed that the deformations introduce micro-cracks and cavities into the material which cause stiffness degradation. The failure criteria are loading criteria and represent threshold variables in the damage model. Non-smooth failure surface allows uncoupled failure.
The geometry of the test article frame was simple and hence it was possible to build a rather regular mesh. The same reference length defined for the composite panel was used.
The riveted and bolted joints were not modeled since it was observed that the benefits of modeling in details the joints were not such to justify the increased model complexity and the required CPU-time; a tied contact type between the Aluminum alloy plate lower surface and the panel upper surface was

defined instead. Point masses were introduced in place of rivets and bolts in effort to reproduce the correct mass distribution. The overall weight of rivets and bolts becomes not negligible when considering all the rivets and bolts together.
The accelerometers were modeled using specific accelerometer elements that allow to measure with accuracy the accelerations in local axis.
Overall, 8471 elements were used to model the test article: 6720 eight-node solid elements for the base frame, 1714 four-node shell elements for the lateral panels and the stiffeners, 37 point masses and 4 dedicated discrete elements type accelerometer [5].
The elastic piecewise linear plasticity material model was adopted to represent the Aluminum alloy behavior. The test article and the skin panel were placed over the fluid surface and the initial velocity equal to the one measured during the test from 0.7 m was imposed to them. A section of the test article model is shown in Fig.9.

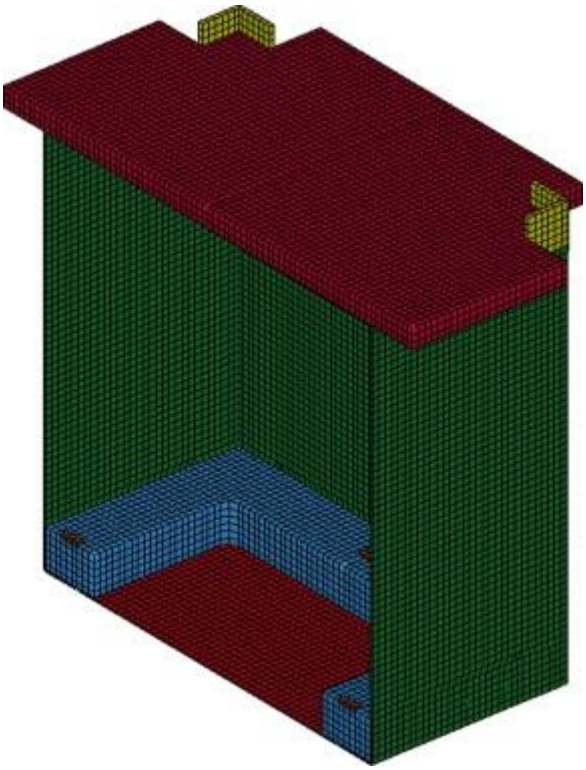

Fig. 9. FE model of the test article.

Numerical models of the fluid region

The water basin used in the tests was a 1.5-m diameter pool. In effort to limit required CPU-time, memory allocation, and to avoid rigid motion of the water, the dimensions of the fluid region in the numerical simulations were smaller than the actual one: the fluid region was modeled as 650 × 650 × 800 mm box.
Reflected waves were avoided imposing non-reflecting silent boundary conditions. The water behavior was reproduced using a previously validated [4] isotropic material characterized by a linear equation of state. A pressure cut-off was defined to roughly model the effect cavitation in the water region. Gravity load was included in the model.
The first water region models were built using the same numbers of nodes for each approach then, after observing the correlation with experimental data, improvements of the models and changes to

the mesh size were introduced according to the behavior of each formulation and to the different sensitivity of each approach.

Lagrangian FE model

The first Lagrangian FE model consisted of 172,970 eight-node solid elements. The mesh was refined below the test article, where the elements belonging to the fluid region have about the same reference length of the elements of the skin panel. Moving along the depth toward the bottom the mesh of the water region becomes progressively coarser.

Silent boundary conditions were imposed using the LS-Dyna non-reflecting boundaries option [5].

The interaction between fluid and structure was reproduced via contact algorithm: in particular, it was defined a bidirectional contact based on penalty method – recommended when the parts in contact have different mechanical properties.

In view of the results of the preliminary simulations it was decided to refine the water region mesh to improve the numerical–experimental correlation.

A new model was created that consisted of 892,080 eight-node solid elements with a reference length reduced to about 4 mm.

ALE model

The ALE mesh consisted of 250,985 eight-node solid elements. The fluid mesh was the same of the Lagrangian model but it was necessary to model an initial surrounding void region where the fluid after the impact could flow. Hence the number of elements is larger. An automatic motion following mass weighted average velocity was imposed to the ALE mesh.

Silent boundary conditions were imposed using the LS-Dyna non-reflecting boundaries option [5].

The interaction between fluid and structure was imposed via coupling algorithm. Since the mesh of the fluid region and the mesh of structure had the same reference length, one point over each coupled Lagrangian surface segment was used. Defining a higher number of points improves the accuracy of the coupling constraint but also increases the stiffness of the coupling interface. A normal direction compression only penalty coupling for shell (without erosion) was defined [5]. The damping factor, which is typical for event involving rigid bodies, was not defined for the penalty coupling, but a coupling leakage control and a mass-based penalty stiffness factor were introduced.

Results of the preliminary simulations run to calibrate the model were satisfactory. Nonetheless, it was decided to refine the mesh to improve the correlation in terms of panel deformations. The new model consisted of 973,504 elements.

SPH model

The first SPH model consisted of 163,863 particles. The accuracy of the SPH model depends on regularity of the particles layout and hence a model characterized by a uniform distribution of the particles was created. The distance between the particles was 12.5 mm.

The boundary conditions at symmetry planes were imposed using a specific boundary condition treatment according to which a set of ghost particles is automatically created by reflecting the particles closest to the boundaries [5]. The ghost particles (which have the same mass, pressure and velocity as the real particles) are included in the neighbors of the real particles and hence contribute to the particle approximation.

A planar infinite rigid wall was created at the bottom of the fluid region to model the presence of the bottom of the tub; the boundary conditions at the water region limits were imposed using finite moving rigid walls. The mass of these rigid walls was calculated considering the part of the water region they substituted. This approach is more general (as it can be adopted in most of the commercially-available programs that implement an SPH solver) and provided good results at a small computational cost [4].

A node-to-surface contact was defined between the SPH particles and the surface of the test articles (modeled using four-node shell elements). The contact constraint was enforced using the penalty method, a suitable choice when the parts in contact have different mechanical properties.
A particle distribution with a distance between particles equal to the resolution of the panel model (6.6 mm) was also investigated the finer model consisted of a uniform grid of 1,100,000 SPH particles. In view of the results of these simulations, it was decided to reduce the number of particles and increase their smoothing length to increase the contact stiffness and hence the impact loads on the panel. The new model consisted of a uniform grid of 36,000 particles with 22 mm spacing.

EFG model

The first EFG model consisted of 36,518 nodes and 166,500 four-node tetrahedral background elements. Tetrahedral background elements were the only available for EFG in LS-Dyna. The distance between the nodes is higher than in the other models: 12 mm in the impact region and 35 mm near the boundaries.
Silent boundary conditions were imposed using the LS-Dyna non-reflecting boundaries option [5].
A node-to-surface contact was defined between the EFG nodes and the surface of the test articles. The contact constraint was enforced using the penalty method, a suitable choice when the parts in contact have different mechanical properties.
The EFG model was subsequently refined to improve the accuracy of the results: 89,964 nodes were used to model the water region. The characteristic length was reduced to 7 mm in the impact region.

Numerical experimental correlation

Numerical results were compared with experimental data with regard to both the impact dynamics captured by the high speed movies and the acquired impact decelerations and deformations.

Impact dynamics

A qualitative index of impact dynamics reproduction has been evaluated by comparing camera frames with numerical simulation frames taken at the same time in terms of water motion and test article sinking behavior. The behavior of both the test article and the fluid region is alike the one captured in the high speed movie for each model realized (Fig.10).
The Lagrangian FE and the ALE models accurately reproduced the behavior of the fluid in terms of water mass bulk motion but not the splash at the sides of the test article. The SPH and the EFG models (in different ways) provided a realistic description not only of the mass bulk motion but also of splattering and spray.

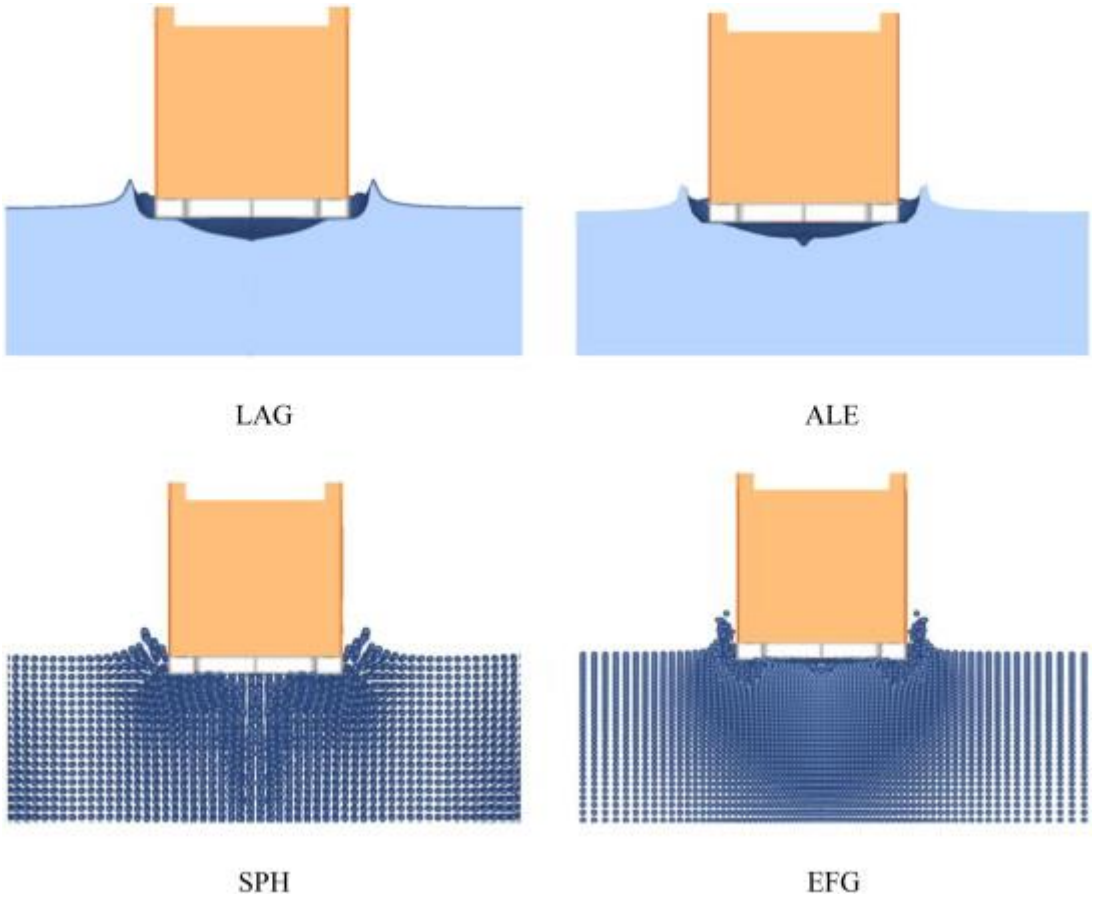

Fig. 10. Frames from the numerical simulations.

Impact decelerations and deformations

The impact deceleration of the test article and the CFRP panel deformation were accurately reproduced by each model used: both the peak value and the event duration were closer to the experimental measurements.

In Tables 2 and 3 every column has two values: the first is relative to the initial water region models whilst the second is related to the new ones.

Model	**N. of elements**	**Peak value**	**Peak duration**	**CPU time [h]**
LAG	172,970	89%	98%	0.5
	892,080	64%	95%	7.8
ALE	250,985	99%	100%	2.5
	973,504	95%	93%	5.5
SPH	163,863	94%	65%	4.0
	36,000	86%	82%	2.0
EFG	36,518	69%	95%	3.5
	89,964	85%	100%	37.5

Table 2. Numerical–experimental correlation on acceleration.

Model	N. of elements	Peak value	Peak duration
LAG	172,970	79%	85%
	892,080	81%	93%
ALE	250,985	73%	88%
	973,504	72%	93%
SPH	163,863	20%	11%
	36,000	71%	83%
EFG	36,518	71%	59%
	89,964	84%	97%

Table 3. Numerical–experimental correlation on deformation.

In Fig. 11the numerical curves are compared with the experimentally measured ones.

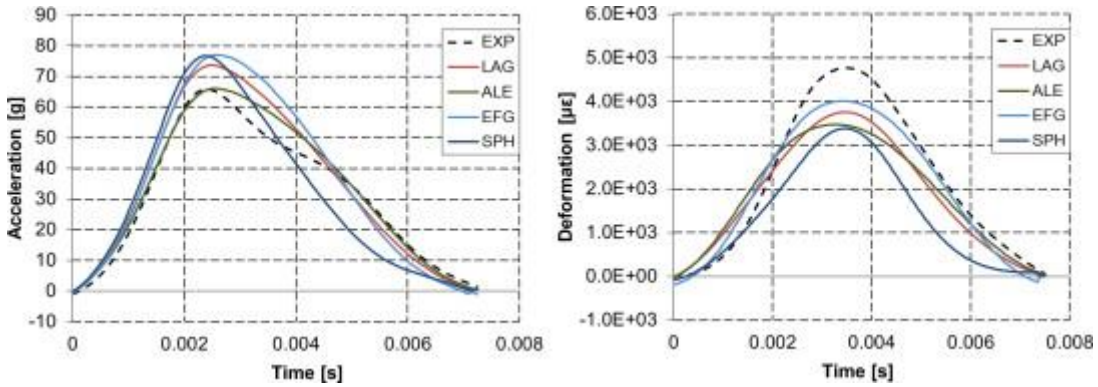

Fig. 11. Numerical–experimental correlation on acceleration (left) and deformation (right).

Required CPU time

The required CPU-time is important for any design-by-analysis procedure. The first 20 ms of the event were simulated using an Intel Core 2 Quad CPU, 2.40 GHz–6 GB RAM PC. The same simulation was run five times and the average required CPU-time is listed in Table 2. The CPU-time was computed in CPU hours for every hundredth of second simulated.

It can be observed that in Lagrangian and EFG improved models, where local refinement has been used instead of global, the explicit method time-step drop caused a higher computational penalty with respect to other formulations.

Panel failure and water inrush

In effort to evaluate the behavior of the composite panel after a structural failure, a water impact at 15 m/s was simulated. Since the failure could be not exactly symmetric it was necessary to model the whole fluid region. In Fig.12 the results of the simulation are shown. The failure was localized in the center part of the panel, where the deformations were larger and propagates from there along the panel.

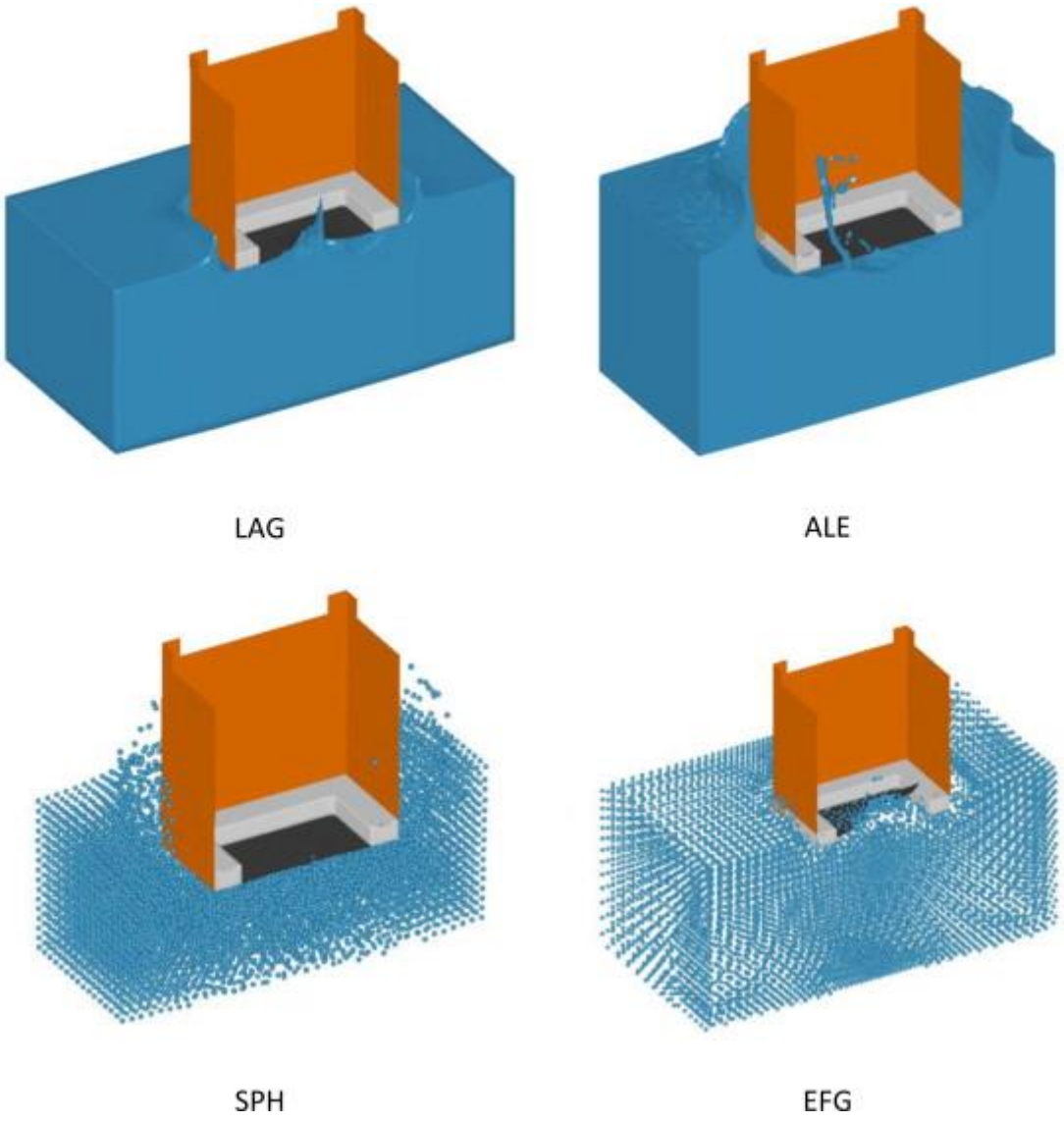

Fig. 12. Frames from the high impact velocity simulations.

The Lagrangian FE model provided a widespread collapse of the panel due not to the effective load transferred to the panel but to the element hourglass. On the other hand the ALE model result seemed more realistic and the failure is localized in the center of the panel. Considering the SPH model, the small deformations obtained produced only a negligible fracture in the center of the CFRP panel. Since it was not possible to use the refined EFG model (because of the excessive memory requirement), the initial coarse model was used: as a result, the failure of the panel was not realistic and it occurred close to the base frame of the test article.

Discussion

The numerical–experimental correlation was globally satisfactory for each model realized both for the acceleration and the deformation. It is relevant to notice the differences between the first and the improved models. The first Lagrangian FE model was more accurate than the refined one because the large deformations of the water elements complicated the tuning of the hourglass coefficients. Nonetheless, when the CPU time becomes higher, performing several analyses is not convenient.
The differences between the first ALE model and the refined one were negligible but each other approach shown significant changes. Nonetheless, because of the limitations in setting the coupling parameters, it was not possible to further improve the correlation on the deformation.

Considering the SPH model, a better correlation was obtained with the coarser model. Indeed increasing the number of SPH particles does not guarantee an improvement of results. Hence finding the more appropriate number of particles and SPH parameters is not trivial.
Considering the EFG models, only the finer model provided satisfactory results but the CPU time was extremely high and the required memory very large. Finally, when considering the failure of the panel, only the ALE approach seemed to provide feasible results and it is consequently necessary to deepen the analysis of this event.

Conclusions

Water impacts of aircrafts and helicopter may turn into a tragic event. In view of that, it is crucial to develop numerical tools to design safer structures with regard to this event.
The outcomes of a research focusing on the impact of composite structure onto water have been presented in this paper. The research consisted of two phases: an experimental phase and a numerical phase.
In the experimental phase, water impact drop tests were carried out and impact decelerations and deformations of a CFRP panel were studied. The tests aimed at collecting data to develop and validate numerical models focusing on impact dynamic and fluid–structure interaction. The dynamics of the event was captured using a high speed camera.
In the numerical phase the tests were reproduced modeling the fluid region with different numerical formulations; two finite elements approaches, Lagrangian and ALE, and two *meshless* formulations, SPH and EFG.
The results obtained with each approach were compared ones to each other and numerical–experimental correlation was evaluated also considering the failure of the CFRP panel and the consequent water inrush.
Finally, pros and cons of each approach, findings and guidelines for further investigations and to study more complex events were obtained.
The Lagrangian approach to fluid region modeling is time effective in terms of model creation and simulations. Models are robust and easy to build. On the negative side, it provides accurate results (close numerical–experimental correlation) only when the fluid deformations are small.
The ALE approach provides satisfactory results and, with the advent of new super-computer and parallel calculation, the required CPU-time is not deemed to represent a limitation to its use. The accuracy of the results obtained relies on the choice of the coupling parameters. Since this choice is not straightforward, the numerical models need to be validated before being employed for the analysis of other similar events.
The SPH approach has the best performance in terms of required calculation time of the simulations. On the other hand, it may be rather time consuming to determine the correct number of particles to achieve a realistic description of the event and close numerical experimental correlation.
The EFG approach provided very accurate results considering both the dynamics and the correlation with the measurements but the CPU-time is relevant.

Acknowledgments

Part of the present research was carried out in cooperation with the GARTEUR AG15 for Helicopter on the “Improvement of SPH methods for application to helicopter ditching”. The authors are thankful to the other members of the Group for the useful discussions and suggestions.

References

1. F.D. Harris, E.F. Kasper, L.E. IselerU.S. civil rotorcraft accidents, 1963 through 1997, NASA STI Program (2000), NASA/TM-2000-209597, USAAMCOM-TR-00-A-006,

2. U.S. Army Aviation Research and Technology ActivityAircraft crash survival design guide, Simula Inc. (December 1989), USAAVSCOM TR 89-D-22 (volumes A–E)
3. J.W. Coltman, A.O. Bolukbasi, D.H. LaananenAnalysis of rotorcraft crash dynamics for development of improved crashworthiness design criteria, U.S. Department of Transportation, Federal Aviation Administration, Technical Center (June 1985), DOT/FAA/CT-85/11
4. M. Anghileri, L.M.L. Castelletti, E. Francesconi, A. Milanese, M. PittofratiRigid body water impact: experimental tests and numerical simulations using SPH method, International Journal of Impact Engineering, 38 (2011), pp. 141-151
5. J.O. HallquistLS-DYNA theoretical manual, Livermore Software Technology Corporation (2006)
6. W. Troesch, C.G. KangHydrodynamic impact loads on three dimensional bodies, 16th Symposium on naval hydrodynamics, Berkeley (July 1986)
7. L.D. Libersky, A.G. Petschek, T.C. Carney, J.R. HippHigh strain Lagrangian hydrodynamics, Journal of Computational Physics (1993)
8. T. Belytschko, Y.Y. Lu, L. GuElement-free Galerkin methods, International Journal of Numerical Methods Engineering, 37 (1994), pp. 229-256